CHAPTER 197

Coastal and Estuarine Hydrodynamic Modeling in Curvilinear Grids

by

Y. Peter Sheng[1], M. ASCE

T.S. Wu[2]

P.F. Wang[2]

ABSTRACT

A time-dependent three-dimensional numerical model of coastal and estuarine circulation, which allows the use of generalized curvilinear grids to resolve the complex shoreline geometry and bathymetry, has been developed. Model formulation is briefly presented, followed by example model applications to such water bodies as Lake Okeechobee, James River and Chesapeake Bay.

INTRODUCTION

Numerical models are routinely used for scientific investigations and management studies of circulation and transport processes in coastal and estuarine waters. However, a number of complexities are associated with the numerical modeling of coastal and estuarine circulation and transport. First of all, the geometry and bathymetry of water bodies are often quite complex (see, for example, Fig. 1). Secondly, circulation and transport in coastal and estuarine waters are generally turbulent and time-dependent, and often three-dimensional. Last but not least, circulation and transport are generally affected by wind, tide, wave, and often density stratification. A thorough discussion of these various aspects and a review of numerous existing hydrodynamic models were presented in Sheng (1986a). This paper focuses on the aspect of complex geometry and bathymetry, and highlights the recent development and application of a curvilinear linear-grid numerical model of coastal and estuarine circulation and transport.

[1]Professor, Coastal and Oceanographic Engineering Department, University of Florida, Gainesville, Florida 32611

[2]Postdoctoral Associate, Coastal and Oceanographic Engineering Department, University of Florida, Gainesville, Florida 32611

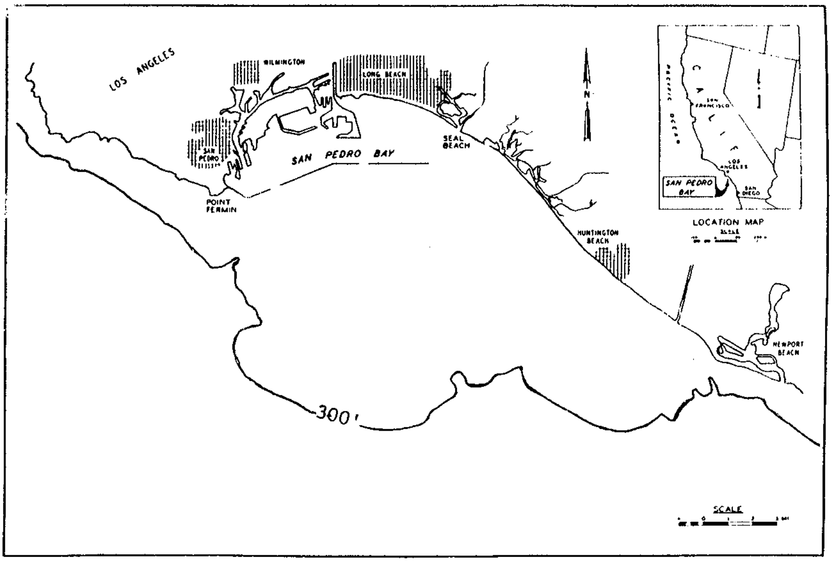

Figure 1. Los Angeles and Long Beach Harbor.

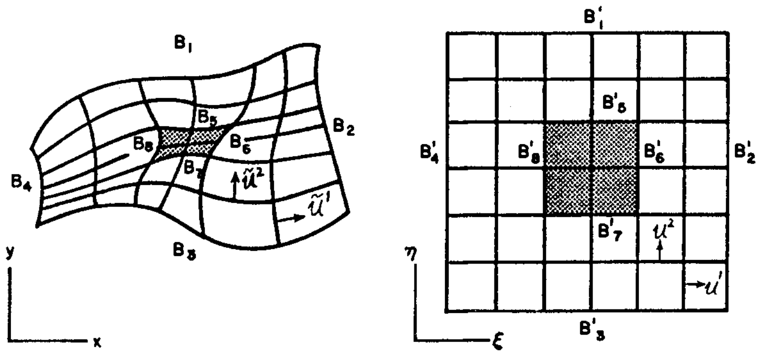

Figure 2(a). Generalized curvilinear (boundary-fitted) grid used in the horizontal directions of the 3-D model.

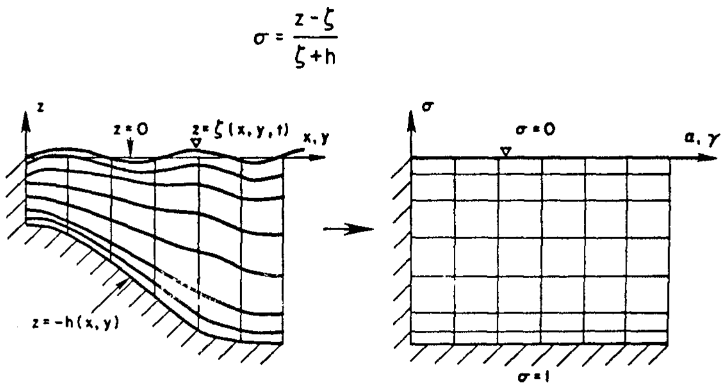

Figure 2(b). Vertical stretching of the coordinates in the 3-D model.

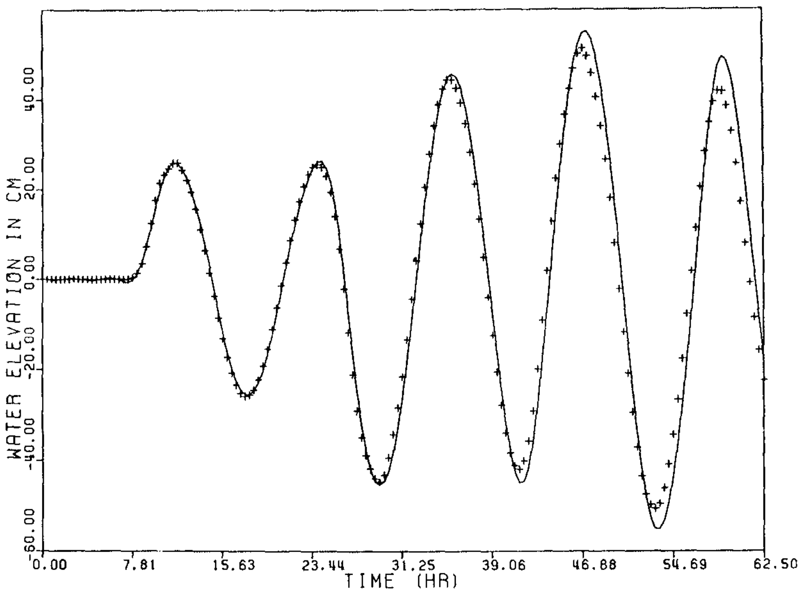

Figure 3. Transient response of water level near the closed end of an initially quiescent basin of 300 km x 29 km x 10 m, subject to a tidal forcing with 1 m amplitude and 12.5 hr period. (—— model results, +++ analytical results)

Traditional finite-difference models use uniform or non-uniform rectangular grid to approximate the complex geometry of water bodies. Consequently, very fine grid is often required to resolve a shoreline or an internal feature such as a structure or navigation channel. As a larger number of rectangular grid points are employed, the "stair-step" model shoreline can better represent the actual shoreline, at the expense of much increased computational cost. To alleviate some of these problems, simple curvilinear grids such as conformal grid (Warnstrath, 1977) and orthogonal curvilinear grid (Bennett and Schwab, 1981) have been used for modeling water bodies where geometries are not so complex. Despite the relative simplicity of these curvilinear grid models, it is extremely difficult (if not impossible) to generate conformal or orthogonal curvilinear grids for most coastal and estuarine water bodies, such as the Los Angeles and Long Beach Harbors shown in Figure 1. Not only is the grid generation process extremely difficult, but the final grid may also be unnecessarily fine in some areas while very coarse in others. In addition, the final grid may not be very smooth. Thus, for coastal and estuarine applications, a hydrodynamic model that can resolve arbitrary shoreline and bathymetry must be developed. Numerical model must be able to accept not only conformal grids or orthogonal grids, but also generalized curvilinear grids which are often non-orthogonal. Such a numerical model will allow the modeler added flexibility in the design of numerical grids with optimal smoothness, resolution, and orthogonality.

This paper presents a generalized curvilinear-grid model for coastal and estuarine circulation and transport. The model resolves the contravariant components of horizontal velocity vectors, thus significantly simplifies the resulting equations of motion and boundary conditions in the transformed grid. In the limiting cases of conformal grids or orthogonal grids, the model equations become substantially simplified.

MODEL FORMULATION

Governing Equations in Curvilinear Grid

The basic circulation and transport model is developed in terms of the contravariant velocity components (u^1 and u^2) in the horizontal directions (x^1 and x^2) and the vertical velocity (ω) in the vertical direction of a σ-stretched (Sheng and Butler, 1982) curvilinear grid (Fig. 2). The basic equations of motion in dimensionless and tensor-invariant forms can be written as (Sheng, 1986b):

$$\zeta_t + \frac{\beta}{\sqrt{g_o}}\frac{\partial}{\partial x^k}\left(\sqrt{g_o}Hu^k\right) + H\frac{\partial \omega}{\partial \sigma} = 0 \tag{1}$$

$$\begin{aligned} \frac{1}{H}\frac{\partial Hu^k}{\partial t} = & - \zeta!^k - g_{nj}\varepsilon^{kj}u^n \\ & - \frac{Ro}{H}\left[(Hu^\ell u^k)_{,\ell} + \frac{\partial Hu^k\omega}{\partial \sigma}\right] \end{aligned} \tag{2}$$

$$
\begin{aligned}
&+ \frac{E_v}{H^2}\frac{\partial}{\partial\sigma}\left(A_v\frac{\partial u^k}{\partial\sigma}\right) + E_H A_H u^k_{,m}!^m \\
&- \frac{Ro}{Fr_d^2}\left[H\int_\sigma^0 \rho!^k d\sigma + H!^k\left(\int_\sigma^0 \rho d\sigma + \sigma\rho\right)\right]
\end{aligned}
$$

where $k = 1$ and 2, $(x^1, x^2) = (\xi, \eta)$ represent the coordinates in the computational domain which is always consisted of uniformly spaced rectangular grid, $\partial/\partial x_k$ is the partial derivative, $g_{\ell n}$ is the metric tensor while g_o is the determinant of the metric tensor, ς is the free surface displacement, $H = h + \varsigma$ is the total depth, u^k is the contravariant velocity component, $\sigma = (z - \varsigma)/(\varsigma + h)$, $(\ )_{,\ell}$ represents the covariant spatial derivative, $!^k$ represents the contravariant spatial derivative, and ε^{kj} is the permutation tensor, $Ro = u_r/fXr$ is the Rossby number, $E_v = A_{vo}/fH^2$ is the vetical Ekman number, $E_H = A_{Ho}/fL^2$ is the lateral Ekman number, $Fr_d = u_r(gD\Delta\rho_o/\rho_o)^{0.5}$ is the densimetric Froude number, $\beta = (Ro/Fr)^2 = gD/f^2L^2$, f is the Coriolis parameter, and (u_r, D, L) represent the reference (velocity, depth, horizontal length).

The above Eq. (2) can be expanded into 2 equations for u^1 and u^2. For example, denoting (u^1, u^2) by (u, v), the following equation represents the momentum equation in the ξ direction (Sheng, 1986b):

$$
\begin{aligned}
\frac{1}{H}\frac{\partial Hu}{\partial t} = &- \left(g^{11}\frac{\partial\varsigma}{\partial\xi} + g^{12}\frac{\partial\varsigma}{\partial\eta}\right) + \frac{g_{12}}{\sqrt{g_o}}u + \frac{g_{22}}{\sqrt{g_o}}v \\
&- \frac{Ro}{H}\left[\frac{\partial}{\partial\xi}(Huu) + \frac{\partial}{\partial\eta}(Huv) + (2D^1_{11} + D^2_{12})Huu\right. \\
&+ \left.(3D^1_{12} + D^2_{22})Huv + D^1_{22}Hvv + \frac{\partial Hu\omega}{\partial\sigma}\right] \\
&+ \frac{E_v}{H^2}\frac{\partial}{\partial\sigma}\left(A_v\frac{\partial u}{\partial\sigma}\right) \\
&- \frac{Ro}{Fr_d^2}\left[H\int_\sigma^0\left(g^{11}\frac{\partial\rho}{\partial\xi} + g^{12}\frac{\partial\rho}{\partial\eta}\right)d\sigma\right. \\
&+ \left.\left(g^{11}\frac{\partial H}{\partial\xi} + g^{12}\frac{\partial H}{\partial\eta}\right)\left(\int_\sigma^0 \rho d\sigma + \sigma\rho\right)\right] \\
&+ E_H A_H \cdot (\text{Horizontal Diffusion of } u)
\end{aligned}
\tag{3}
$$

where D^i_{jk} represents the Christoffel symbol of the second kind:

$$
\begin{aligned}
D^i_{jk} &= g^{in}D_{njk} \\
&= \frac{1}{2}g^{in}(g_{nj:k} + g_{nk:j} - g_{jk:n})
\end{aligned}
\tag{4}
$$

The above equation appears to be more complicated than the momentum equation in a Cartesian grid with (x, y, σ) or (x, y, z) as coordinates. Most of the terms are doubled, while nonlinear and lateral diffusion terms are more than doubled. However, if an orthogonal grid is used, the following equation will result from Eq. (3):

$$
\begin{aligned}
\frac{1}{H}\frac{\partial Hu}{\partial t} = & - g^{11}\frac{\partial \zeta}{\partial \xi} + \frac{g_{22}}{\sqrt{g_o}}v \\
& - \frac{Ro}{H}\left[\frac{\partial}{\partial \xi}(Huu) + \frac{\partial}{\partial \eta}(Huv) + \frac{\partial Hu\omega}{\partial \sigma}\right] \\
& + \frac{E_v}{H^2}\frac{\partial}{\partial \sigma}\left(A_v\frac{\partial u}{\partial \sigma}\right) \\
& - \frac{Ro}{Fr_d^2}\left[H\int_\sigma^0 g^{11}\frac{\partial \rho}{\partial \xi}d\sigma + g^{11}\frac{\partial H}{\partial \xi}\left(\int_\sigma^0 \rho d\sigma + \sigma\rho\right)\right] \\
& + E_H A_H\left(g^{11}\frac{\partial^2 u}{\partial \xi^2} + g^{22}\frac{\partial^2 u}{\partial \eta^2}\right)
\end{aligned}
\tag{5}
$$

As indicated before, such simplified equation cannot be used unless the shoreline geometry is so simple such an orthogonal grid can be generated. Even then, the numerically computed metric coefficients, which represent the geometric effects in the transformed equations of motion, do not necessarily guarantee the satisfication of conservation laws in the discrete system.

The transport equations for temperature, salinity, and sediment concentration are simpler and can be written as:

$$
\begin{aligned}
\frac{1}{H}\frac{\partial H\phi}{\partial t} = & \frac{E_v}{Pr_v}\frac{\partial}{H^2\partial \sigma}\left(K_v\frac{\partial \phi}{\partial \sigma}\right) \\
& - \frac{Ro}{H\sqrt{g_o}}\left(\frac{\partial\sqrt{g_o}Hu\phi}{\partial \xi} + \frac{\partial\sqrt{g_o}Hu\phi}{\partial \eta} + \frac{\partial\sqrt{g_o}H\omega\phi}{\partial \sigma}\right) \\
& + \frac{E_H K_H}{Pr_H}\left(g^{11}\frac{\partial^2\phi}{\partial \xi^2} + 2g^{12}\frac{\partial^2\phi}{\partial \xi\partial \eta} + g^{22}\frac{\partial^2\phi}{\partial \eta^2}\right)
\end{aligned}
\tag{6}
$$

where ϕ can be temperature (T), salinity (S), or suspended sediment concentration (C), (Pr_v, Pr_H) represent the vertical and lateral turbulent Prandtl numbers, and (K_v, K_H) are the dimensionless vertical and horizontal turbulent diffusivities.

Other Model Features

The above system of equations are solved in conjunction with the proper boundary conditions at the free surface, the bottom, and the lateral boundaries. At the bottom, the velocity profile asymptotically approaches that of the law-of-the-wall, with a drag coefficient which depends on the bottom roughness.

Turbulence parameterization used in the present model is similar to the one described in Sheng (1987). While the horizontal turbulent eddy coefficients are prescribed as uniform values which decrease with the grid spacing, the vertical eddy coefficients are determined from simplified versions of a second-order closure model of turbulent transport (Sheng and Chiu, 1986; Sheng and Villaret, 1988).

Numerical Algorithm

To allow efficient solution of the 3-D model, the mode-splitting technique described in Sheng et. al. (1978) and Sheng and Butler (1982) is also used here. Vertically-integrated equations obtained by integrating Eqs. (1) and (2) represent the so-called "external mode", while the internal mode consists of equations obtained by subtracting the vertically-averaged equations from the u and v equations. An ADI scheme, which is somewhat more complicated than that for the Cartesian equations, is used for the external mode of the present model. Either two-time-level or three-time-level scheme can be used for the time integration of the 3-D model.

The numerical model described above constitutes the main body of a flow code, CH3D. In addition to CH3D, a grid generation code based on the elliptic grid generation technique (Thompson and Johnson, 1985) and a preprocessor code (Sheng, 1986) which computes the metric coefficients must also be used when solving practical problems.

At the present time, we do not adjust the grid during a particular model simulation. Adaptive grid technique, which allows the adjustment of grid resolution according to the evolution of dynamic flow, is being developed (Sheng and Luo, 1988).

Model Applications

Numerous model simulations have been performed. Model applications to a number of idealized basins were presented in Sheng (1987). Additional model sensitivity tests have been performed. For example, Figure 3 shows the transient response of an initially quiescent rectangular basin (300 Km x 29 Km x 10 m) to a suddenly imposed tidal forcing with 1 m amplitude and 12.5 hr period. Since no diffusion or bottom friction was used in the model, the model results faithfully simulated the analytically computed transient response which consists of higher harmonics in addition to the forcing harmonic.

Model application to the James River estuary (Fig. 4) produced mean tides which agreed well with data, both in terms of amplitude (Fig. 5) and phase shift (Fig. 6). Model application to the Chesapeake Bay (Fig. 7) produced results which compared well with mean tides. Significant spatial variation is found in the model computed velocity field, which is being compared with measured data now. The same basic model is being applied to the upper Chesapeake Bay (Johnson, 1988).

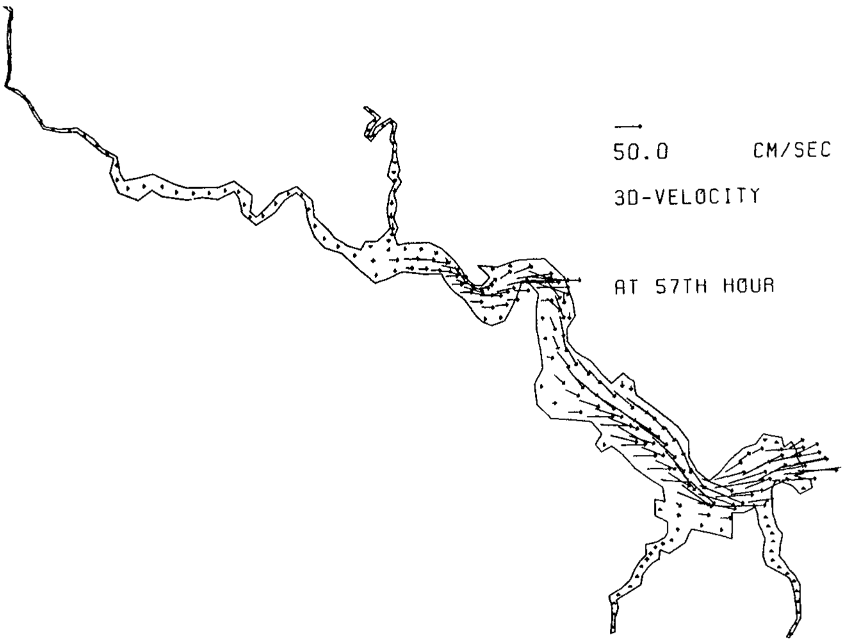

Figure 4. Near-surface current in the James River driven by a M_2 tide of 38 cm amplitude at the open boundary.

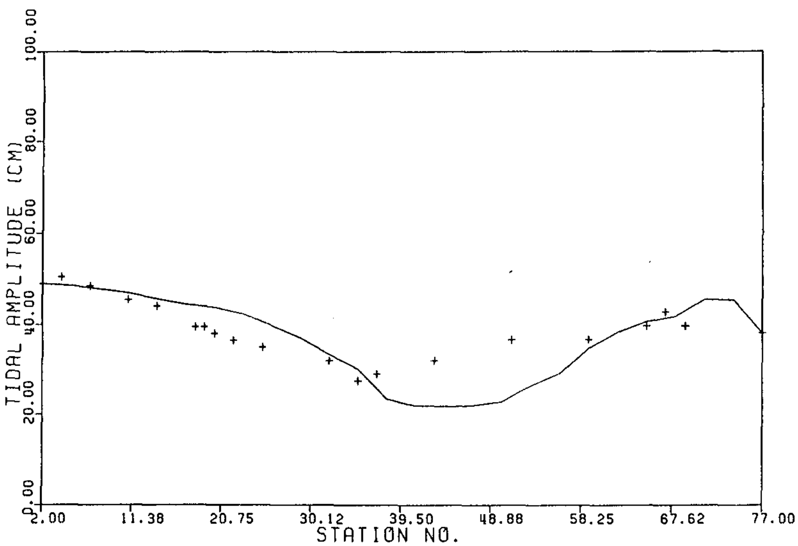

Figure 5. Mean M_2 tidal amplitude in the James River (—— model results, +++ data). Amplitude at open boundary = 38 cm.

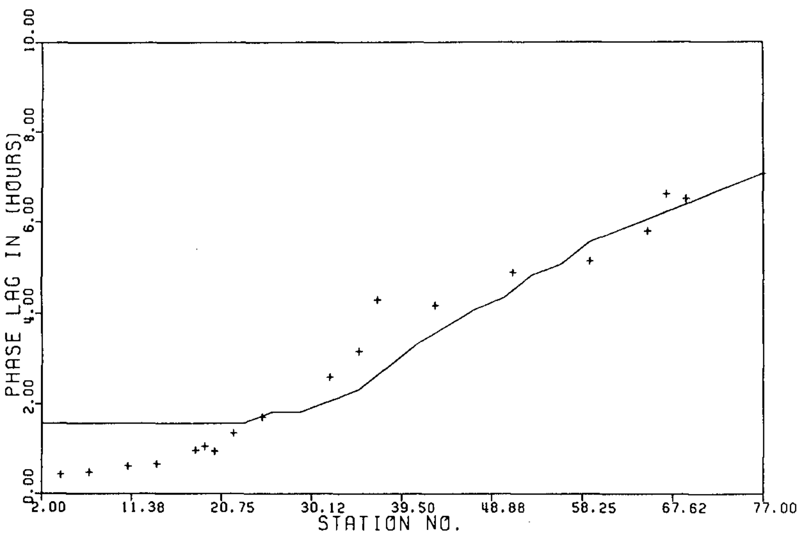

Figure 6. Mean M_2 tidal phase lag in the James River (—— model results, +++ data).

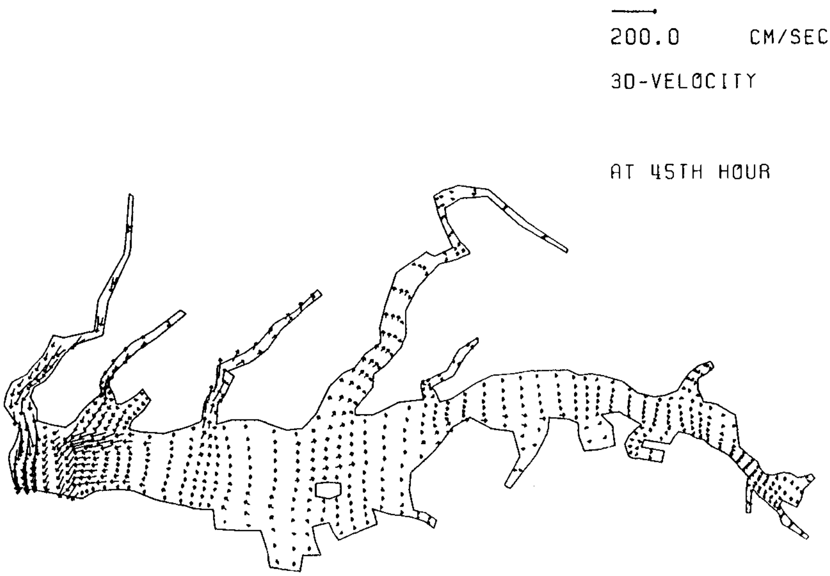

Figure 7. Near-surface current in the Chesapeake Bay driven by a M_2 tide of 60 cm amplitude.

Model application to Lake Okeechobee showed that, despite the shallowness of the lake (average depth of 3m), significant return flow is produced near the bottom due to a 5 ms^{-1} wind from the east (Figs. 8 and 9). The vertically-averaged velocity field clearly showed the existence of 2 topographically induced circulation gyres.

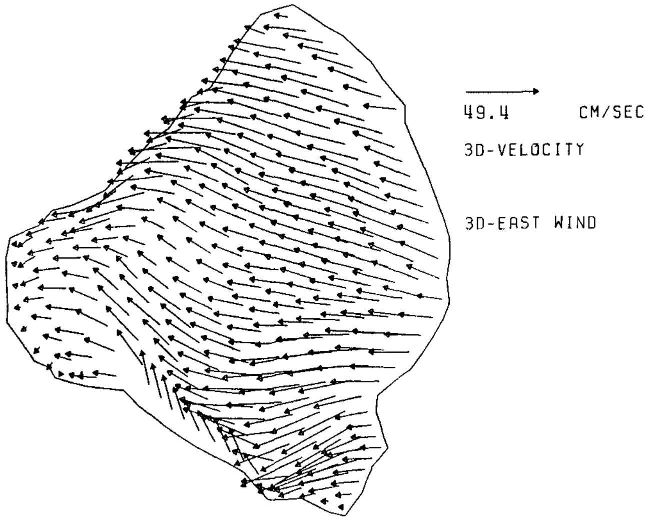

Figure 8. Near-surface wind-driven currents in Lake Okeechobee due to a wind of 5 m/sec from the east.

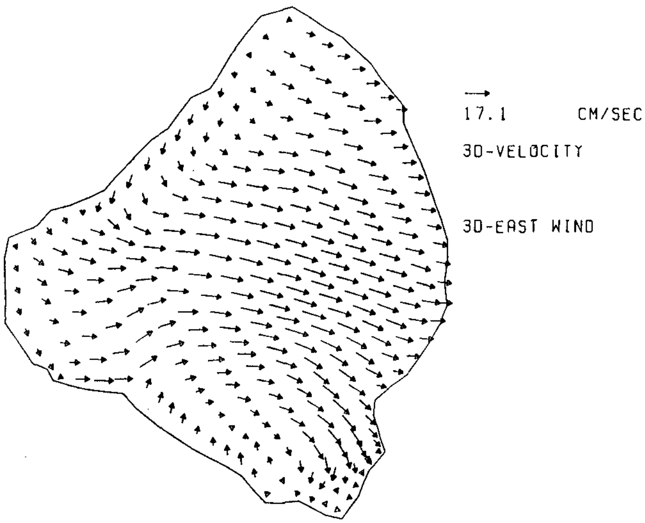

Figure 9. Near-bottom wind-driven currents in Lake Okeechobee due to a wind of 5 m/sec from the east.

ACKNOWLEDGEMENT

Supports from U.S. Army Engineer Waterways Experiment Station, Virginia Institute of Marine Science, and South Florida Water Management District are acknowledged.

REFERENCES

1. Bennett, J.R. and D.J. Schwab, 1981: "Calculation of the Rotational Normal Modes of Oceans and Lakes with General Orthogonal Coordinates", Journal of Comp. Phys., vol. 44, pp. 359-376.

2. Johnson, B.H., 1988: "An Approach for Modeling the Upper Chesapeake Bay", Proc. of the 1988 National Conference on Hydraulic Engineering, ASCE, pp. 588-93.

3. Sheng, Y.P., 1986a: "Finite-Difference Models for Hydrodynamics of Lakes and Shallow Seas", in Physics-Based Model of Lakes, Reservoirs, & Impoundments (W.G.Gray, ed.), ASCE, pp. 146-228.

4. Sheng, Y.P., 1986b: "A Three-Dimensional Mathematical Model of Coastal, Estuarine and Lake Currents Using Boundary-Fitted Grid", ARAP Technical Report No. 585, Aeronautical Research Associates of Princeton/California Research and Technology/Titan Systems, Princeton, N.J.

5. Sheng, Y.P., 1987: "On Modeling Three-Dimensional Estuarine and Marine Hydrodynamics", in Three-Dimensional Models of Marine and Estuarine Dynamics (J.C.J. Nihoul and B.M. Jamart, eds.), Elsevier Oceanography Series, Elsevier, pp. 35=54.

6. Sheng, Y.P., W. Lick, R.T. Gedney, and F.B. Molls, 1978: "Numerical Computation of Three-Dimensional Circulation in Lake Erie: A Comparison of a Free-Surface Model and a Rigid-Lid Model", J. Phys. Oceanog., Vol. 1, pp. 713-27.

7. Sheng, Y.P. and H.L. Butler, 1982: "Modeling Coastal Currents and Sediment Transport", Proc. of the 18th ICCE, ASCE, pp. 1127-48.

8. Sheng, Y.P. and S.S. Chiu, 1981: "Tropical Cyclone Generated Currents", Proc. of the 20th ICCE, ASCE, pp. 737-51.

9. Sheng, Y.P. and C. Villaret, 1988: "Modeling the Effect of Suspended Sediment Stratification on Bottom Exchange Processes", Submitted to the Journal of Geophysical Research.

10. Thompson, J.F. and B.H. Johnson, 1985: "Development of an Adaptive Boundary-Fitted Coordinate Code for Use in Coastal and Estuarine Areas", Misc. Paper HL-85-5, U.S. Army Engineer Waterways Experiment Station, Vicksburg, MS.

11. Warnstrath, J.J., 1977: "Nearshore Numerical Storm Surge and Tidal Simulation Model", T.R. H-77-17, U.S. Army Engineer Waterways Experiment Station, Vicksburg, MS.